

# WiCAU: Comprehensive Partial Adaptation with Uncertainty-aware for WiFi-based Cross-environment Activity Recognition

Wei Cui, Keyu Wu, Min Wu, Xiaoli Li, and Zhenghua Chen\*

**Abstract**—Recently, WiFi-based human activity recognition (HAR) has emerged as a promising technique for human-computer interactions, owing to its widespread availability and non-invasiveness. However, deploying WiFi-based HAR systems in new environments often results in performance degradation. Existing WiFi-based HAR systems across different environments typically assume identical category spaces between the source and target, an assumption challenged by practical scenarios. In this paper, we present WiCAU, a comprehensive adaptation with uncertainty-awareness for WiFi-based HAR across environments, designed to tackle the challenges of environments with unequal category spaces—a scenario known as Partial Domain Adaptation (PDA). Different from conventional PDA methods that usually focus on training the feature extractor to align feature distributions or implement separate reweighting models to adjust source domain feature weights, WiCAU integrates feature alignment and source data reweighting to mitigate the risk of negative transfer. It also introduces an uncertain complement entropy to effectively handle uncertainty within the source environment. Moreover, WiCAU employs a hybrid network that combines wavelet analysis with deep neural networks to capture both the temporal and spatial dynamics present in WiFi Channel State Information (CSI) data. WiCAU’s superior performance in PDA scenarios for HAR is demonstrated through comprehensive experiments with both self-built and publicly available datasets.

**Index Terms**—Human Activity Recognition, Channel State Information, WiFi, Partial Domain Adaptation, Negative Transfer.

## I. INTRODUCTION

Accurate and efficient human activity recognition (HAR) is crucial for facilitating personalized and context-aware services within human-computer interaction. It can be utilized in a wide range of applications, including healthcare monitoring, assisted living, and smart homes. As a result, HAR has garnered significant attention in recent years [1].

Numerous techniques have been proposed for HAR, involving diverse modalities such as visual images, wearable sensors, and wireless signals [2], [3]. Among these, WiFi-based HAR has garnered significant attention due to its distinct advantages, including device-free sensing and privacy preservation [4], [5]. WiFi-based HAR leverages the ubiquitous WiFi infrastructures

to capture and analyze variations in WiFi signals introduced by human activities [6]. Unlike wearable sensors that require individuals to carry devices, WiFi-based methods enable activity recognition in a device-free manner. Moreover, WiFi signals can penetrate walls and other obstacles, allowing for the capture of activity information without directly capturing visual or personal identifying details of individuals. Consequently, WiFi-based HAR offers an additional advantage in terms of privacy preservation.

To effectively analyze changes in WiFi signal characteristics and classify activities, existing WiFi-based HAR techniques employ various machine learning techniques such as support vector machine, hidden markov model (HMM), random forest (RF), as well as deep learning techniques such as the convolutional neural network (CNN) and recurrent neural network (RNN) [7]. These algorithms are utilized to learn complicated patterns and relationships present in the extracted features derived from WiFi signals, enabling activity classification.

However, in wireless-based HAR, the same behavior performed in different environments can have distinct data distributions due to environmental variations. This poses a challenge for traditional WiFi-based recognition approaches, leading to reduced performance and accuracy across diverse environments. To address this challenge, domain adaptation algorithms have been developed to mitigate the effects of environment-specific variations and improve the generalization capability of behavior recognition models. Nevertheless, traditional domain adaptation (DA) methods in WiFi-based HAR rely on aligning the labeled source domain samples with the unlabeled target domain samples, assuming that both domains share the same category space. However, achieving identical category spaces between two domains in practical WiFi-based HAR scenarios is often unrealistic, particularly when the target domain represents only a subset of the classes present in the source domain. This situation is known as the Partial Domain Adaptation (PDA) problem. The presence of the PDA problem poses a significant challenge when using traditional domain adaptation approaches to address the domain shift in WiFi-based activity recognition, as these techniques may struggle to effectively adapt the models due to the mismatch in category spaces between the domains. Consequently, the performance of the activity recognition system may be degraded.

Typically, PDA presents additional challenges compared to regular closed-set domain adaptation due to the presence of categories that exist exclusively in the source domain. This situation causes a feature mismatch when aligning distribu-

Wei Cui, Keyu Wu, Min Wu, Xiaoli Li and Zhenghua Chen are with Institute for Infocomm Research (I2R), Agency for Science, Technology and Research (A\*STAR).

\* indicates the corresponding author. Email: chen\_zhenghua@i2r.a-star.edu.sg

This research is supported by the Agency for Science, Technology and Research (A\*STAR) under its Career Development Award (Grant No. C210112046).

tions, leading to negative transfer and degrading the learning performance of the target domain. In order to address the problem of negative transfer, current PDA methods commonly employ reweighting strategies on the source domain sample to reduce the influence of source-only classes. These methods train the feature extractor using a reweighted distribution alignment loss defined on the target and reweighted source data. However, these reweighted feature distribution alignment methods lack robustness in handling the uncertainties associated with source data weights, potentially assigning non-zero weights to source-only-class data in the alignment losses. Moreover, previous PDA methods have predominantly focused on enhancing feature transferability by developing various domain alignment strategies, often overlooking the aspect of feature discriminability. These methods typically rely on conventional cross-entropy loss in the labeled source domain to learn features. However, these approaches can introduce confusion and uncertainty propagation issues in the target domain, as the source classes are not equally separated from each other [8]. Furthermore, existing PDA methods are primarily designed for the computer vision domain and do not fully leverage the specific features provided by WiFi-based HAR, such as temporal and spatial Channel state information (CSI) data of WiFi. These features are essential for accurately recognizing human activities in WiFi signals.

In this paper, we propose WiCAU (Comprehensive Adaptation with Uncertainty-aware), a novel approach for WiFi-based HAR that addresses the challenges of domain shift and uncertainty propagation when adapting to the target domain. Specifically, in contrast to traditional PDA methods that either align feature distributions or employ separate reweighting models, our proposed approach takes a comprehensive approach. We simultaneously adapt the feature extractor and reweight the source domain data features to reduce the negative transfer and improve the adaptability of the model.

Furthermore, to tackle the issue of uncertainty propagation in the source domain, we introduce an uncertain complement entropy. This entropy measure takes into account the uncertainty present in the source domain data and helps improve the classification performance of the model during the adaptation process. By addressing uncertainty propagation, our approach enhances the model's robustness and accuracy in recognizing activities in the target domain. Additionally, to exploit the temporal and spatial relations in the CSI data, we introduce an integrated network that combines wavelet and deep neural network architectures as the feature extractor. This integration allows us to effectively capture and utilize the rich information present in CSI data. The proposed WiCAU can be applied in various practical domains, including human-computer interaction, security and surveillance, and smart living. For example, WiCAU can be used to monitor individuals' daily activities and optimize energy usage and automation in smart homes by adjusting lighting, temperature, and security systems in response to occupants' activities. The proposed WiCAU enables health monitoring across varying environments, ensuring accurate human activity recognition even when the available labeled data only partially aligns with the target domain. To sum up, this paper makes the following contributions:

- (1) We develop the WiCAU method, which comprehensively addresses the challenges of negative transfer and uncertainty propagation in WiFi-based HAR by jointly aligning feature distributions, optimizing source domain data weights, and incorporating the uncertain complement entropy.
- (2) We introduce an integrated network that combines wavelet analysis and deep neural networks to capture the information inherent in CSI data. By leveraging the complementary strengths of both, our approach can improve the performance of CSI-based HAR systems.
- (3) We perform extensive experiments on various datasets, using diverse datasets, including both self-created and publicly accessible WiFi-based HAR datasets. The experimental results show the efficiency of our proposed approach, achieving state-of-the-art performance in HAR tasks.

## II. RELATED WORK

### A. Cross-domain WiFi-based HAR

In recent years, WiFi-based HAR has witnessed significant advancements through the application of various deep learning methodologies, including CNNs, RNNs, and transformer architectures. These techniques have proven to be adept at automatically extracting features from fine-grained CSI data, offering a promising avenue for WiFi-based HAR research. Deng *et al.* introduced a residual module coupled with depth-wise separable convolution in their work [9]. Meanwhile, the Long Short-Term Memory (LSTM), renowned for its capacity to model temporal dependencies, found utility in HAR tasks leveraging WiFi CSI data [10]. Yang *et al.* designed a WiFi-based gesture recognition model, fusing the strengths of CNNs and RNNs [11]. Their approach used CNNs to extract spatial features while employing RNNs to capture the temporal dynamics in gestures. Similarly, Wang *et al.* explored the fusion of CNN and LSTM to achieve reliable activity recognition using CSI [12]. Zou *et al.* introduced an AE-LRCN framework [13], which incorporates an autoencoder module, a CNN module, and an LSTM module for WiFi-based HAR. Furthermore, they explored EfficientFi using a quantized representation learning framework to reduce communication overhead for WiFi-based HAR. Zhang *et al.* [6] introduced a fusion deep model that integrates semantic features extracted from CNN with temporal features derived from bidirectional gated recurrent units (BGRU). Li *et al.* employed transformer architectures for WiFi-based HAR, presenting the Two-stream Convolution Augmented Human Activity Transformer (THAT) model [14].

Though deep learning models exhibit strong fitting capacities, these WiFi-based HAR models using these techniques often perform well within well-defined domains but degrade when confronted with new and varying environments. This limitation stems from WiFi-based HAR environments that may undergo significant dynamics, leading to the challenge of domain shifts. To address this issue, domain-adaptive methods for WiFi-based HAR have been proposed. Pioneering efforts [15], [16], [17] mainly adopted the adversarial training framework as a means to address the domain shift. These approaches

operate on the premise that unlabeled data can be accessed within the target domain. These approaches have proven to be effective in mitigating the influence of domain-specific variations. However, it has been observed by Zhou *et al.* [18] that these methods do not use the entirety of the available data. Typically, they either concentrate on unlabeled data or labeled data within the target domain. To address this limitation, they introduced the Target-Oriented Semi-Supervised (TOSS) domain adaptation approach for WiFi-based HAR. This approach employs both labeled and unlabeled data in the target domain. It's noteworthy that the aforementioned methods primarily focus on addressing closed-set domain adaptation, thus overlooking the partial domain adaptation scenarios in WiFi-based HAR.

### B. Partial Domain Adaptation

Domain adaptation in transfer learning aims to minimize the discrepancy between source and target domains by learning domain-invariant features, thereby reducing the labeling cost in the target domain. Approaches can be categorized into two types: statistical feature-based methods and adversarial-based methods. Statistical feature-based methods utilize techniques such as maximum mean discrepancy (MMD) [19], [20] or higher-order moment matching [21], [22] to align the distributions between domains. Adversarial-based methods, on the other hand, employ domain discriminators to train feature extractors that confuse domain differentiation, enabling the capture of domain-invariant representations for effective knowledge transfer [23], [24].

However, in more realistic and general scenarios of DA, it is common to encounter situations where the label space of the target domain is a subset of the source domain. This setting also is referred to as PDA. The pioneering work by Hsu *et al.* [25] tackles the challenge of imbalanced scenarios, where there exists a discrepancy in the label distribution between the source and target domains. This work has paved the way for subsequent research in this field. The Selective Adversarial Network (SAN) proposed by Cao *et al.* [26] tackles the challenge by employing a multi-discriminator approach. It assigns weights to different discriminators, allowing for selective emphasis on source-only classes during the adaptation process. In contrast, Importance Weighted Adversarial Nets (IWAN) [27] employs a single domain discriminator and assigns weights to each source sample based on its probability of belonging to the target domain. Similarly, the Deep Residual Correction Network (DRCN) introduced by Li *et al.* [28] presents a weighted class-wise matching approach that aims to align the target data with the most relevant classes in the source domain. The Example Transfer Network (ETN) proposed by Cao *et al.* [29] takes a distinct approach by simultaneously learning domain-invariant representations across domains. ETN employs a weighting strategy to assess the transferability of source examples. Previous methods often match the entire source domain to the target domain, leading to negative transfer due to the presence of source-negative classes that do not exist in the target domain. To address this issue, Discriminative Partial Domain Adversarial

Network (DPDAN) [30] introduces a hard binary weighting algorithm. This algorithm assigns high weights to positive classes and near-zero weights to negative classes, effectively reducing negative transfer. In a similar vein, Gu *et al.* [31] proposed an Adversarial Reweighting (AR) approach that utilizes adversarial learning to determine the weights of the source domain data. Moreover, Balanced and Uncertainty-Aware Approach for Partial Domain Adaptation (BA<sup>3</sup>US) [8] tackles the challenge of asymmetric label distributions by augmenting the target domain and effectively transforming it into a problem resembling unsupervised domain adaptation (UDA). In general, the PDA methods mentioned above either focus on training the feature extractor to align the feature distributions of the reweighted source and target domain data or employ a separate reweighting model to adjust the weights of the source domain data features. In comparison, our proposed method takes a comprehensive approach by simultaneously adapting the feature extractor and reweighting the source domain data features. This dual strategy aims to effectively reduce the negative transfer in PDA by jointly aligning the feature distributions and optimizing the weights of the source domain data.

## III. PROPOSED COMPREHENSIVE ADAPTATION

In this section, we provide a detailed explanation of the WiCAU framework. We begin by introducing the definitions and notations used in the PDA scenarios for WiFi-based HAR.

### A. Channel State Information

We employ CSI measurements as our wireless input data. CSI provides detailed channel information between the WiFi transmitter and receiver, offering fine-grained information for analysis. In an Orthogonal Frequency Division Multiplexing (OFDM) system, the transmission channel typically comprises multiple subcarriers. Considering a scenario with  $N_t$  transmitters and  $N_r$  receivers, and each channel containing  $N_k$  subcarriers, the channel model for the  $k$ -th subcarrier is expressed as:

$$\mathbf{b} = \mathbf{x}_k \times \mathbf{a} + \mathbf{n} \quad (1)$$

where  $\mathbf{b} \in \mathbb{C}^{N_r}$  represents the received wireless signal vectors,  $\mathbf{a} \in \mathbb{C}^{N_t}$  denotes the corresponding transmitted wireless signal vectors, and  $\mathbf{n}$  represents additive white gaussian noise. The channel matrix for the  $k$ -th subcarrier is denoted as  $\mathbf{x}_k \in \mathbb{C}^{N_t \times N_r}$ . The complete CSI can be represented as a multi-dimensional matrix  $\mathbf{x} \in \mathbb{C}^{N_t \times N_r \times N_k}$ .

### B. Problem Setting

We are given a labeled dataset  $\mathcal{D}_s = \{x_i^s, y_i^s\}_{i=1}^{n^s}$ ,  $x^s \in \mathbb{R}^d$  in the source environment, where  $x_i^s \in \mathbb{R}^d$  represents the collected CSI data and  $y_i^s \in \mathcal{Y}^s$  indicates the corresponding activity label for  $x_i^s$ . Additionally, we have an unlabeled target environment dataset  $\mathcal{D}_t = \{x_j^t\}_{j=1}^{n^t}$ , where  $x_j^t \in \mathbb{R}^d$  represents the collected wireless signals in the target environment. It is important to note that the label space for the target environment, denoted as  $\mathcal{Y}^t$ , is a subset of the label space for the

source environment, i.e.,  $\mathcal{Y}^t \subset \mathcal{Y}^s$ . This is in contrast to the closed-set domain adaptation setting where  $\mathcal{Y}^t = \mathcal{Y}^s$ . Our aim is to learn a deep neural network to predict the activity  $y^t \in \mathcal{Y}^t$  of the corresponding CSI data  $x^t$  in the new environment.

In Partial Domain Adaptation, wireless-based HAR encounters the challenge of negative transfer. This challenge arises from the discrepancy in joint distributions, particularly in the asymmetry of marginal label distributions within PDA. This asymmetry exposes source-only classes to the risk of being inappropriately matched with target classes, thereby creating negative transfer. To address this issue, popular PDA methods frequently employ re-weighting mechanisms to differentiate source-only classes and facilitate positive transfer across shared classes between domains. Conventionally, PDA solutions have focused on aligning feature distributions through the adaptation of the feature extractor. However, in situations where the domain discrepancy is significant, the predictions from the source classifier on target domain data can exhibit uncertainty. This uncertainty can lead to non-zero probabilities of classifying target data as source-only classes. Consequently, re-weighting source classes based on classifier outputs may inadvertently introduce “noisy” weights. As noise levels increase, alignment performance, as measured by alignment losses, diminishes markedly and can even lead to significantly degraded results.

To address this challenge, we introduce a novel comprehensive adaptation approach. This approach not only involves adapting the feature extractor through reweighted distribution alignment but also aligns the distributions of source and target domain features using adversarial learning. The overall framework is depicted in Fig. 1, comprising four key modules: a shared feature extractor  $F$ , a reweighting model  $W$ , a classifier  $C$ , and a domain discriminator  $D_a$  for adapting the feature extractor.

### C. Feature Distribution Alignment with Reweighting Model

As mentioned in [29], source domain data that belongs to the shared class  $y^t$  exhibits closer proximity to target domain data compared to those from the source-only class  $y^s / y^t$ . In order to reduce the influence of source-only data, our approach introduces a weight learning mechanism by maximizing the similarity between the weighted source domain distribution and the target domain distribution. This weight learning process is realized through adversarial learning, involving interactions between a domain discriminator  $D_r$  and the similarity measurement, as illustrated in Fig. 1.

Within the reweighting model, the domain discriminator  $D_r$  is characterized by its parameters  $\theta_{d_r}$ , and the domain-shared feature extractor  $F$  is parameterized by  $\theta_f$ . This feature extractor yields extracted features,  $z_i^s = F(x_i^s; \theta_f)$  and  $z_j^t = F(x_j^t; \theta_f)$ , derived from source and target wireless signals, respectively. The empirical distribution of target domain data is expressed as  $P_t = \frac{1}{n^t} \sum_{j=1}^{n^t} \delta(z_j^t)$ , wherein  $\delta(\cdot)$  signifies the Dirac delta function. Our approach involves weights, denoted as  $\mathbf{w} = \{w_1, w_2, \dots, w_{n^s}\}^T$ , which specify the relative significance of source domain data, subject to the constraint  $\sum_{i=1}^{n^s} w_i = n^s$ . These weights facilitate the

creation of a reweighted source domain distribution,  $P_s = \frac{1}{n^s} \sum_{i=1}^{n^s} w_i \delta(z_i^s)$ . To quantify the similarity between source and target probability distributions, we adopt the Wasserstein distance [32], chosen for its superior continuity in distribution learning. The Wasserstein distance is represented as  $W(P_s, P_t) = \min_{\pi \in \Pi} \mathbb{E}_{(P_s, P_t) \sim \pi} \|P_s - P_t\|$ , where  $\|\cdot\|$  denotes the  $l_2$  norm, and  $\Pi$  signifies the set of couplings of  $P_s$  and  $P_t$ . We learn the weights  $\mathbf{w}$  by maximizing the similarity between the reweighted source feature distribution  $P_s$  and the target feature distribution  $P_t$ , namely,

$$\max_{\mathbf{w}} (1 - W(P^s(\mathbf{w}), P^t)) \quad (2)$$

In parallel, we employ adversarial training where the weights  $\mathbf{w}$  remain fixed, while the domain discriminator within reweighting model  $D_r$  is trained to minimize its average output on the target domain, while maximizing its average output on the source domain, thereby distinguishing the source and target domains, which can be defined as:

$$\min_{\theta_{d_r}} \left( \frac{1}{n^s} \sum_{i=1}^{n^s} w_i \log [1 - D_r(z_i^s)] + \frac{1}{n^t} \sum_{j=1}^{n^t} \log [D_r(z_j^t)] \right) \quad (3)$$

This optimization process ensures that the weights  $\mathbf{w}$  are learned to maximize feature distribution similarity while the domain discriminator within reweighting model  $D_r$  distinguishes between source and target domains effectively.

### D. Adapting Feature Extractor by Reweighted Distribution Alignment

In addition to aligning the source weighted feature distribution with the target feature distribution, our approach also involves adapting the feature extractor through reweighted distribution alignment. This process is illustrated in Fig. 1. The weighted features, derived from the reweighting model, are input into the classifier denoted as  $C(x_i^s; \theta_c)$  and the domain discriminator for feature extractor adaptation denoted as  $D_a(\cdot; \theta_{d_a})$ . The objective is to learn the parameters  $\theta_f$  of the feature extractor  $F$  by maximizing the loss of the domain discriminator  $d_a$ , while simultaneously learning the parameters  $\theta_{d_a}$  of the domain discriminator  $D_a$  by minimizing its loss. Furthermore, the loss of the source classifier  $C(x_i^s; \theta_c)$  is minimized to ensure reduced source domain classification errors. The objective for reweighted distribution alignment can be expressed as:

$$\min_{\theta_f, \theta_c} \max_{\theta_{d_a}} \mathcal{L}_{adv}(\theta_f, \theta_{d_a}) + \mathcal{L}_{cls}(\theta_f, \theta_c) \quad (4)$$

where  $\mathcal{L}_{adv}$  represents the adversarial loss as defined in Eq. (5), while  $\mathcal{L}_{cls}$  stands for the classification loss incurred by source labeled samples, which will be elaborated in the subsequent subsection (III-D2).

$$\begin{aligned} \mathcal{L}_{adv}(\theta_f, \theta_{d_a}) = & \frac{1}{n^s} \sum_{i=1}^{n^s} w_i \log [D_a(F(x_i^s))] \\ & + \frac{1}{n^t} \sum_{j=1}^{n^t} \log [1 - D_a(F(x_j^t))] \end{aligned} \quad (5)$$

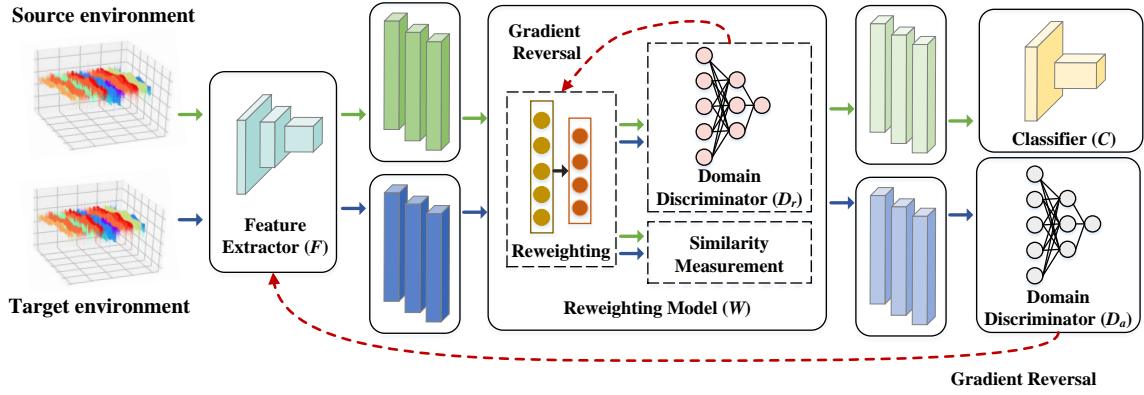


Fig. 1: Architecture of our proposed network.

1) *Deep wavelet based feature extractor*: CSI measurements obtained from commercial WiFi often suffer from significant noise caused by dynamic range variations and fluctuations within high-dimensional channels. These fluctuations arise from various sources, including multipath interference and radio signal disruptions, and are observed even in stable environments. To address such challenges, wavelet analysis has found extensive utility in wireless signal denoising. Wavelet analysis offers the advantages of multidomain analysis for wireless signal, allowing signal examination in both the time and frequency domains, and fine-grained multiscale analysis, which provides a comprehensive understanding of signal characteristics across multiple scales. The conventional wavelet approach involves a multi-step process, including the transformation of data into distinct frequency intervals, followed by targeted denoising of high-frequency components. This transformation, exemplified by methods like Discrete Wavelet Transform (DWT), encompasses filtering and downsampling operations. However, these traditional DWT procedures necessitate the development of bespoke techniques to attain optimal performance, leading to system recalibration upon environmental changes. Meanwhile, deep learning methods have gained considerable attention due to their capacity to recognize hidden patterns within wireless signals. In a majority of studies, these methods achieve state-of-the-art results in wireless-based HAR in an end-to-end manner. For example, in previous research [33], [10], [14], it has been consistently observed that employing advanced deep learning techniques, such as LSTM and CNN, yields superior accuracy compared to simpler shallow learning algorithms like RF and HMM. It's worth noting, that widely adopted deep learning architectures such as CNNs and RNNs do not incorporate filtering mechanisms, which may result in degrading the noise-robustness of networks.

In response to this challenge, we introduce a deep wavelet-based feature extractor, a combination of DWT and deep neural networks, to enhance signal feature representation for noise-resistant signal processing in wireless signal based HAR.

The foundation of our proposed feature extractor lies in the DWT which operates as follows. Given a time-windowed series of CSI measurements, denoted as  $\mathbf{x} = \{x_i\}$ , collected from a single subcarrier, we first feed it to the conventional

convolution layer to get the representatives  $\mathbf{l} = \{l_i\}$ . Then we employ the DWT to decompose this signal into two components: a low-frequency component,  $\mathbf{l}_1 = \{l_{1,d}\}$ , and a high-frequency component,  $\mathbf{h}_1 = \{h_{1,d}\}$ . The decomposition process is mathematically represented as follows:

$$\begin{cases} l_{1,d} = \sum_i s_{i-2d}^l l_i \\ h_{1,d} = \sum_i s_{i-2d}^h h_i \end{cases} \quad (6)$$

where  $\mathbf{s}^l = \{s_d^l\}_{d \in \mathbb{Z}}$  and  $\mathbf{s}^h = \{s_d^h\}_{d \in \mathbb{Z}}$  represent the low-pass and high-pass filters of an orthogonal wavelet. This DWT process, outlined in Eq. (6), consists of filtering and downsampling operations.

With the matrix and vector, the mathematical expressions in Eq. (6) can be rewritten as Eq. (7).

$$\begin{cases} \mathbf{l}_1 = \mathbf{s}^l \mathbf{l} \\ \mathbf{h}_1 = \mathbf{s}^h \mathbf{l} \end{cases} \quad (7)$$

Practically, during backward propagation, we differentiate Eq. (7), resulting in the following gradients:

$$\begin{cases} \frac{\partial \mathbf{l}_1}{\partial \mathbf{l}} = (\mathbf{s}^l)^T \\ \frac{\partial \mathbf{h}_1}{\partial \mathbf{l}} = (\mathbf{s}^h)^T \end{cases} \quad (8)$$

For the signal reconstruction, a critical step is the filtering of high-frequency components. Notably, high-frequency elements are conventionally treated as noise within wireless signals. Thus, considering the unique characteristics of CSI data, our approach chooses to directly remove these high-frequency elements. To be specific, our feature extractor leverages wavelets with finite filters. We employed a CNN with four layers as the backbone, wherein the commonly used downsampling is replaced by DWT with the low-frequency component. This modification effectively reduces the size of the feature maps.

In summary, our deep wavelet-based feature extractor can effectively remove high-frequency components and denoise the signal while preserving its low-frequency core.

2) *Classifier with anti-uncertain propagation*: In the partial domain adaptation framework, it is customary to employ the cross-entropy loss, denoted as  $\mathcal{L}_{ce}$ . This loss, used for the source classifier, is usually defined as follows [34], [23]:

$$\mathcal{L}_{ce}(\theta_f, \theta_c) = \frac{1}{n^s} \sum_{i=1}^{n^s} w_i l_{ce}(C(F(x_i^s)), y_i^s) \quad (9)$$

where  $l_{ce}(\cdot, \cdot)$  denotes the softmax cross-entropy loss.

However, traditional domain adaptation methods utilizing this classifier loss primarily focus on enhancing feature transferability through diverse domain alignment strategies. They rely solely on the conventional cross-entropy loss within the labeled source domain for feature learning, often overlooking the crucial aspect of feature discriminability. Meanwhile, CSI data is susceptible to variations induced by human activities, typically exhibits high discriminability across different environments or subjects (i.e., domains). Consequently, although traditional DA techniques may mitigate domain shifts for Cross-Domain CSI-based HAR, they might compromise classifier performance on target data. This issue particularly rooted in the unequal separation of source classes from each other, which subsequently triggers the propagation of confusion, or uncertainty, into target predictions. This phenomenon is also recognized as the ‘‘uncertainty propagation problem.’’ To illustrate, consider the cross-entropy loss  $l_{ce}(\hat{y}, y) = -\sum_i y_i \log(\hat{y}_i)$ , it essentially leverages information solely from the ground-truth class while disregards information from other incorrect classes. For instance, if the source output is [0.60, 0.35, 0.05], it is more uncertain than [0.60, 0.20, 0.20], yet both situations yield the same cross-entropy loss.

To solve this problem, we propose a classifier with anti-uncertain propagation loss, which employs an additional complement entropy aiming for uniformly low prediction scores regarding incorrect classes for labeled source samples. To better mitigate uncertainty, we further pay more attention to the uncertain samples that own smaller cross-entropy loss. The complement anti-uncertain entropy objective  $\mathcal{L}_{ace}$  is defined as below:

$$\begin{aligned} \mathcal{L}_{ace}(\theta_f, \theta_c) &= \frac{1}{n^s \log(K-1)} \sum_{i=1}^{n^s} m(y_i^s) l_{ace}(C(F(x_i^s)), y_i^s) \\ l_{ace}(\hat{y}_i^s, y_i^s) &= (1 - \hat{y}_q)^\gamma \sum_{j \neq q} \frac{\hat{y}_j}{1 - \hat{y}_q} \log\left(\frac{\hat{y}_j}{1 - \hat{y}_q}\right) \end{aligned} \quad (10)$$

where  $\gamma$  is a hyperparameter that modulates the emphasis on uncertain samples, and  $q$  denotes the index of the ground-truth class. This formulation effectively tackles the uncertainty propagation problem by giving due consideration to the confidence levels of predictions for each class. Consequently, our classifier loss  $\mathcal{L}_{cls}$  is defined as a weighted combination of  $\mathcal{L}_{ace}$  and  $\mathcal{L}_{ce}$ :

$$\mathcal{L}_{cls}(\theta_f, \theta_c) = \alpha \mathcal{L}_{ace}(\theta_f, \theta_c) + \beta \mathcal{L}_{ce}(\theta_f, \theta_c) \quad (11)$$

where  $\alpha$  and  $\beta$  are hyperparameters that allow us to control the influence of each loss component in the final objective. Thus, the objective of Eq. (4) can be rewritten as:

$$\min_{\theta_f, \theta_c} \max_{\theta_{da}} \mathcal{L}_{adv}(\theta_f, \theta_{da}) + \alpha \mathcal{L}_{ace}(\theta_f, \theta_c) + \beta \mathcal{L}_{ce}(\theta_f, \theta_c) \quad (12)$$

By combining the complement entropy-based loss with the traditional cross-entropy loss, our classifier effectively mitigates the uncertainty propagation problem, enhancing the robustness and reliability of the classifier in cross-domain CSI-based HAR.

### E. Training Algorithm

During the training of the network, we adopt an alternating optimization strategy involving the network parameters  $(\theta_f, \theta_c, \theta_{da}, \theta_{dr})$  and the weight vector  $\mathbf{w}$  while keeping the other components constant. The weight vector  $\mathbf{w}$  is initialized with  $w_i = 1$  for all  $i$ . The training process alternates between two main procedures:

1) Updating  $\theta_f$  and  $\theta_c$  with fixed  $\mathbf{w}$

With  $\mathbf{w}$  held constant, we update the parameters  $\theta_f$  and  $\theta_c$  using Eq. 12. As Eq. 12 represents a min-max optimization problem, we iteratively optimize the parameters  $\theta_f, \theta_c$  and  $\theta_{da}$  while keeping the other one fixed. Initially, we freeze the parameters for the feature extractor and classifier,  $\theta_f, \theta_c$ , and optimize the parameters of the discriminator within the reweighting model,  $\theta_{da}$ , to maximize the objective. Then, with the discriminator fixed, we optimize the feature extractor and classifier.

2) Updating  $\mathbf{w}$  with Fixed  $\theta_f$  and  $\theta_c$

With fixed  $\theta_f$  and  $\theta_c$ , we extract features from all training data in both the source and target domains and adjust the weights  $\mathbf{w}$  by training the reweighting model. This weight learning process leverages adversarial learning, and we iteratively optimize the weights  $\mathbf{w}$  and the parameters  $\theta_{dr}$  of the discriminator for feature extractor adaptation while keeping the other constant. Initially, according to Eq. 2, we fix  $\mathbf{w}$  and optimize  $\theta_{dr}$  to maximize the similarity between the reweighted source feature distribution and the target feature distribution. Subsequently, with the discriminator fixed, we fine-tune  $\mathbf{w}$  using optimization techniques as described in [31], [35] (as shown in Eq. 3).

## IV. EXPERIMENTS

### A. Experimental Setup

1) *Datasets*: In our experimental evaluation, we employed two distinct datasets: our self-built dataset, *WiHAR*, and a publicly accessible dataset named *CSLOS* [36].

For *WiHAR*, we selected three typical environments (i.e., an office room, a pantry room, and a seminar room, their layouts are shown in Fig. 2) to collect data that are close to real-world scenarios. The data acquisition process involved the use of two laptops equipped with Intel5300 network cards, serving as the hardware platform for signal reception. In each of the selected environments, a signal transmitter (Tx) and receiver (Rx) were positioned at a fixed distance of 3.5 meters, and their antenna height was maintained at 1.2 meters. To capture high-quality WiFi signal data, we equipped both the Tx and Rx terminals with three gain antennas, resulting in a total of six external antennas. The Intel 5300 wireless network card was instrumental in obtaining data from 30 sub-carriers, effectively creating a 30-channel CSI dataset. Throughout the

data collection phase, we maintained a sampling rate of 500Hz, resulting in the generation of 2000 packets per sample.

Our *WiHAR* dataset contains seven behavior types, including “stand still,” “jump,” “bend over,” “run,” “sit,” “walk,” and “wave hand.” To ensure the robustness and diversity of our dataset, seven individuals participated in the data collection process for each of the seven behavior types within each environment. Remarkably, each participant performed each behavior a total of 101 times. The selection of individuals for participation was carried out by taking into account variations in height, weight, size, gender, and other distinctive characteristics. Overall, our dataset contains a total of 4949 samples for each environment, ensuring the comprehensive coverage of human actions in various settings.

*CSLOS* involved three distinct environments: a research laboratory, a university hallway, and an NLOS indoor environment. For the laboratory environment, experiments were conducted within the confines of a laboratory space. The hallway environment simulated a dynamic scenario, with students and university employees moving in the vicinity of the hallway alongside the subjects performing experiments. 30 subjects volunteered for the experiments in each of the three environments. Each subject performed five experiments with 12 activities, including “Sit still”, “Fall down from sitting position”, “Lie down”, “Stand still”, “Fall down from standing position”, “Walk from transmitter to receiver”, “Turn”, “Walk from receiver to transmitter”, “Turn in a different direction”, “Stand up”, “Sit down”, “Pick a pen from the ground”. Each experiment was repeated 20 times for each environment.

2) *Methods for Comparison and Training Details*: We compared our proposed approach *WiCAU* with six widely recognized models, including supervised WiFi-based HAR model, domain adaptation methods, and partial domain adaptation approaches. Here, we provide a brief overview of each of these methods:

**CNN [37]**: [37] utilizes a Convolutional Neural Network to analyze channel data and infer user behaviors. In our experiments, we trained the CNN model solely on source samples and subsequently evaluated its performance on the target domain data.

**Domain-adversarial Neural Network (DANN) [23]**: DANN is a typical unsupervised domain adaptation technique that employs a gradient reversal layer to train a domain classifier in an adversarial manner while optimizing a feature extractor network.

**Adversarial Discriminative Domain Adaptation (ADDA) [38]**: ADDA is a state-of-the-art unsupervised domain adversarial adaptation model in computer vision that effectively mitigates the effects of domain shift by combining adversarial learning with discriminative feature learning.

**Entropy conditioning variant of Conditional Domain Adversarial Network (CDAN+E) [39]**: CDAN+E introduces two innovative conditioning strategies for domain adaptation. Multilinear conditioning captures cross-covariance between features and classifier predictions for enhanced discriminability, while entropy conditioning controls classifier prediction uncertainty to ensure transferability.

**Partial Adversarial Domain Adaptation (PADA) [40]**: PADA is designed for partial domain adaptation, specifically addressing negative transfer by down-weighting data from outlier source classes during the training of both the source classifier and domain discriminator.

**BA<sup>3</sup>US [8]**: BA<sup>3</sup>US is a state-of-the-art PDA technique that employs a strategic selection of source samples to enhance the target domain during the domain alignment process. This technique is aimed at achieving class symmetry across distinct domains.

All the methods were implemented in Python 3.8 using PyTorch 1.11 with CUDA 11.7. The implementation was carried out on an NVIDIA 3060 GPU with 12 GB of memory. We utilized the stochastic gradient descent (SGD) algorithm for optimization, setting the learning rate to  $1e-4$ . The batch size for training was 64. The architecture of the discriminator  $D_r$  and  $D_a$  consisted of three fully connected layers with 1024, 1024, and 1 nodes, respectively. In the deep wavelet-based feature extractor with a CNN of four layers, the strides were set to 2, and the kernel size was  $5 \times 5$ . The Rectified Linear Unit (ReLU) activation function was applied. To maintain fairness in our comparative analysis, the same discriminator architecture was used in all models where necessary.

## B. Results

1) *Overall results*: For each dataset, we conducted experiments across six domain adaptation settings, each involving the adaptation from one environment to another. Considering that each dataset encompasses three distinct environments, this results in a total of six unique adaptation scenarios. We randomly selected 5 activities to build the target domain for both datasets. The experimental results of our proposed method alongside several state-of-the-art domain adaptation techniques on *WiHAR* and *CSLOS* are present in Tables I and II.

Overall, in comparison, traditional supervised CNN exhibited limited adaptability, with average accuracies of 23.4% (*WiHAR*) and 31.4% (*CSLOS*). Significantly, across various domain adaptation methods, our proposed *WiCAU* consistently delivered superior accuracy on both the *WiHAR* and *CSLOS* datasets. This highlights its outstanding performance in effectively tackling the challenge of domain shift.

With the *WiHAR* dataset, we observed substantial improvements in action recognition accuracy compared to existing methods. Remarkably, our proposed *WiCAU* achieved an average accuracy of 80.8%, outperforming the second-best performing approach, BA<sup>3</sup>US, by a significant margin of 6.4%. Specifically, when examining the results from different domain pairs (1→2, 2→1, 2→3, 3→2, 3→1, 1→3), our approach consistently outperformed other methods. In the 2→1 scenario, our accuracy reached an impressive 86.4%, showcasing the superiority of our model in adapting to challenging domain shifts. The results in all other domain pairs further support the efficacy of our method. The performance of previous state-of-the-art PDA techniques such as PADA and BA<sup>3</sup>US is better than traditional domain adaptation techniques ADDA, DANN, and CDAN+E, demonstrating their effectiveness in handling partial domain adaptation tasks.

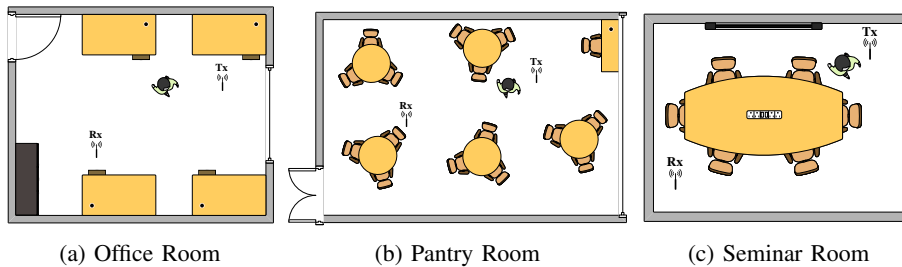


Fig. 2: The layouts for three indoor environments

TABLE I: Accuracy (%) on *WiHAR* for partial domain adaptation.

Accuracy (%)	<i>WiHAR</i>						Avg
	1 → 2	2 → 1	2 → 3	3 → 2	3 → 1	1 → 3	
CNN [37]	16.3	27.1	25.6	30.9	23.9	16.6	23.4
ADDA [23]	44.1	32.3	60.8	52.1	44.4	47.3	46.8
DANN [38]	71.1	66.3	46.5	56.4	76.9	74.2	65.2
CDAN+E [39]	75.2	64.2	55.4	74.6	67.9	67.6	67.5
PADA [40]	78.9	75.6	72.4	71.0	73.7	73.2	74.1
BA <sup>3</sup> US [8]	72.9	73.9	72.2	75.1	77.1	74.9	74.4
WiCAU (Ours)	<b>84.9</b>	<b>86.4</b>	<b>82.6</b>	<b>77.3</b>	<b>78.2</b>	<b>75.1</b>	<b>80.8</b>

TABLE II: Accuracy (%) on *CSLOS* for partial domain adaptation.

Accuracy (%)	<i>CSLOS</i>						Avg
	1 → 2	2 → 1	2 → 3	3 → 2	3 → 1	1 → 3	
CNN [37]	30.4	28.3	26.6	23.7	38.1	41.2	31.4
ADDA [23]	33.3	23.7	36.6	34.5	43.7	39.5	35.2
DANN [38]	37.0	20.4	29.5	32.9	39.5	55.8	35.8
CDAN+E [39]	33.7	28.7	29.5	30.4	36.2	44.5	33.8
PADA [40]	44.5	27.0	22.5	35.0	41.6	56.1	37.8
BA <sup>3</sup> US [8]	43.3	34.1	40.4	44.1	45.2	56.2	43.9
WiCAU (Ours)	<b>60.0</b>	<b>34.2</b>	<b>41.2</b>	<b>53.3</b>	<b>61.2</b>	<b>62.9</b>	<b>52.1</b>

On the *CSLOS* dataset, our method also demonstrates remarkable domain adaptation capabilities. We achieved an average accuracy of 52.1%, which is notably higher than the results obtained by competing methods. In particular, it outperforms the second-best approach, BA<sup>3</sup>US, by a significant margin of 8.2%. This dataset presents its unique challenges due to only 5 activities selected in the target domain, whereas the source domain has 12 activities, making domain adaptation crucial. Our method consistently outperforms others across various domain pairs, highlighting its robustness. In particular, the 1→3 scenario yielded an accuracy of 62.9%, indicating the effectiveness of our approach in adapting human action recognition models to different environments.

2) *Ablation study*: In the ablation study, we aimed to assess the individual contributions of several key components proposed in our approach, including feature distribution alignment with reweighting model, reweighted distribution alignment with feature extractor adaptation, deep wavelet-based feature extraction, and the anti-uncertain propagation module. Table III presents the results of this study. It’s important to note that we conducted these tests by substituting the ablated component with an existing alternative method. Specifically, we used a four-layer CNN to replace our deep wavelet-based feature extraction, employed the framework for reweighting distribution alignment in PDA [8] as a substitute for our reweighting model, and integrated the framework for feature distribution alignment in PDA [31] in place of our reweighted

distribution alignment with feature extractor adaptation.

From Table III, we can see that removing the deep wavelet-based feature extraction component resulted in a noticeable decrease in accuracy across all adaptation settings. On average, this ablation led to a 1.6 percentage point decline in accuracy. This suggests that the deep wavelet-based feature extraction method contributes to recognizing domain-specific patterns, which is important for effective adaptation. Moreover, the exclusion of the anti-uncertain propagation module led to a 1.0 percentage point reduction in accuracy across all adaptation scenarios. This shows the anti-uncertain propagation module plays a role in handling data uncertainty, and its presence improves the model’s robustness.

Besides, ablating the distribution alignment with the reweighting model resulted in a significant decrease in accuracy. On average, there was a 3.9 percentage point reduction in accuracy. This highlights the importance of this module in aligning the distributions with weights between the source and target domains, a fundamental aspect of PDA. Removing the reweighted distribution alignment with feature extractor adaptation component also led to a notable decrease (i.e., 3.3%) in accuracy across all adaptation settings. This module’s role in adapting the feature extractor to align the distributions for PDA is evidently crucial.

3) *Accuracy with varying number of target classes*: In our exploration of the impact of varying target class numbers, we conducted an assessment of our proposed method with



TABLE III: Ablation study results compared with the full WiCAU model using WiHAR dataset

Accuracy(%)	1 → 2	2 → 1	2 → 3	3 → 2	3 → 1	1 → 3	Avg	$\Delta$
WiCAU	84.9	86.4	82.6	77.3	78.2	75.1	80.8	-
= Deep wavelet based feature extraction	83.7	85.5	81.3	76.2	76.3	73.9	79.2	-1.6
= Anti-uncertain propagation module	84.1	85.8	81.3	76.1	77.5	74.2	79.8	-1.0
= Distribution alignment with reweighting model	81.7	82.6	79.7	72.9	73.5	71.2	76.9	-3.9
= Reweighted distribution alignment with feature extractor adaptation	81.2	84.4	79.2	74.3	76.4	69.6	77.5	-3.3

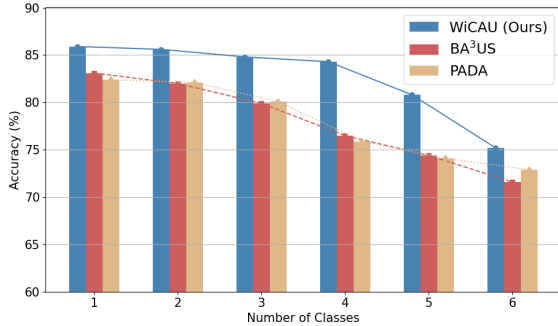


Fig. 3: Accuracy with the varying number of target classes.

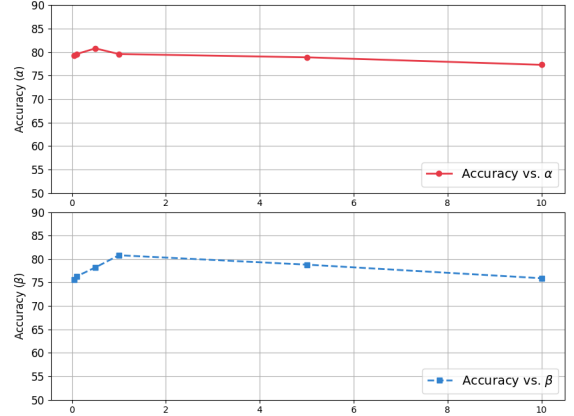
two other PDA approaches. The range of target class counts spanned from 1 to 6 (7 activity classes in the source domain). From the results shown in Fig. 3, we can observe that all methods start with heightened accuracy for a single target class and then experience a gradual decline as the number of target classes increases. However, our method, WiCAU, exhibits consistently the highest accuracy across different numbers of target classes. This observation strongly indicates that WiCAU excels in WiFi-based HAR partial domain adaptation scenarios where there is a mismatch in the label space between the source and target domains.

4) *Parameter sensitivity*: We conducted a sensitivity analysis of the parameters  $\alpha$  and  $\beta$  in Eq. 12 of our WiCAU model using the WiHAR dataset. We systematically varied these parameters over a range of values (0.05, 0.1, 0.5, 1, 5, 10) to observe their impact on model performance. The results, as depicted in Fig. 4, reveal that our model’s performance is relatively stable across different values of  $\alpha$  and  $\beta$ . Notably, the accuracy remains consistent in the vicinity of 1 and 5, indicating that our method is not particularly sensitive to these parameter values.

5) *Performance for closed-set domain adaptation*: In this section, we further investigate the effectiveness of the proposed WiCAU for vanilla closed-set domain adaptation. We compare our method with other state-of-the-art methods using the WiHAR dataset. Table IV presents the accuracy results for closed-set domain adaptation. As demonstrated, our proposed method achieves a competitive average accuracy and ranks among the top two when compared to the other methods. This outcome verifies the effectiveness of our approach even in the scenario of closed-set domain adaptation.

## V. CONCLUSION

The ability to recognize activities across varying WiFi environments presents a formidable challenge for WiFi-based HAR. Traditional domain adaptation methods for WiFi-based

Fig. 4: Accuracy vs.  $\alpha$  and  $\beta$ .

HAR typically confine their scope to closed-set domain adaptation scenarios, a limitation that can manifest as challenges when the source and target domains encompass different activity categories. Furthermore, current Partial Domain Adaptation techniques are mainly developed for the computer vision field and do not consider the unique attributes provided by WiFi-based HAR. To address these challenges, we proposed WiCAU, an innovative approach for WiFi-based HAR. WiCAU comprehensively tackles negative transfer and uncertainty propagation by simultaneously adapting the feature extractor and reweighting source domain data features. Our extensive experiments, spanning various datasets, including self-built, publicly available datasets, have demonstrated WiCAU’s superior performance. In the future, we plan to investigate the integration of wireless signals with other sensing modalities, including wearable devices or visual images, to significantly enhance HAR performance and robustness across diverse scenarios.

## REFERENCES

- [1] L. M. Dang, K. Min, H. Wang, M. J. Piran, C. H. Lee, and H. Moon, “Sensor-based and vision-based human activity recognition: A comprehensive survey,” *Pattern Recognition*, vol. 108, p. 107561, 2020.
- [2] E. Ramanujam, T. Perumal, and S. Padmavathi, “Human activity recognition with smartphone and wearable sensors using deep learning techniques: A review,” *IEEE Sensors Journal*, vol. 21, no. 12, pp. 13 029–13 040, 2021.
- [3] Z. Sun, Q. Ke, H. Rahmani, M. Bennamoun, G. Wang, and J. Liu, “Human action recognition from various data modalities: A review,” *IEEE transactions on pattern analysis and machine intelligence*, 2022.
- [4] M. G. Moghaddam, A. A. N. Shirehjini, and S. Shirmohammadi, “A wifi-based method for recognizing fine-grained multiple-subject human activities,” *IEEE Transactions on Instrumentation and Measurement*, 2023.
- [5] Z. Zhou, F. Wang, and W. Gong, “i-sample: Augment domain adversarial adaptation models for wifi-based har,” *ACM Transactions on Sensor Networks*, 2023.

TABLE IV: Accuracy (%) on WiHAR for closed-set domain adaptation.

Accuracy (%)	WiHAR						
	1 → 2	2 → 1	2 → 3	3 → 2	3 → 1	1 → 3	Avg
CNN	22.2	30.3	20.9	31.5	28.7	21.0	25.8
ADDA	64.6	71.5	67.4	65.0	66.9	55.2	65.1
DANN	73.8	85.1	77.8	69.6	74.9	61.1	73.7
CDAN+E	<b>75.9</b>	<b>86.3</b>	<b>78.7</b>	<b>71.9</b>	<b>75.5</b>	<b>63.2</b>	<b>75.3</b>
PADA	72.1	73.9	68.2	65.8	70.1	62.8	68.8
BA <sup>3</sup> US	60.2	63.1	59.3	64.7	67.2	58.6	62.2
WiCAU (Ours)	<b>75.6</b>	<b>78.8</b>	<b>76.8</b>	<b>72.0</b>	<b>74.2</b>	<b>65.7</b>	<b>73.8</b>

- [6] Y. Zhang, Q. Liu, Y. Wang, and G. Yu, "Csi-based location-independent human activity recognition using feature fusion," *IEEE Transactions on Instrumentation and Measurement*, vol. 71, pp. 1–12, 2022.
- [7] J. Yang, Y. Xu, H. Cao, H. Zou, and L. Xie, "Deep learning and transfer learning for device-free human activity recognition: A survey," *Journal of Automation and Intelligence*, vol. 1, no. 1, p. 100007, 2022.
- [8] J. Liang, Y. Wang, D. Hu, R. He, and J. Feng, "A balanced and uncertainty-aware approach for partial domain adaptation," in *European conference on computer vision*. Springer, 2020, pp. 123–140.
- [9] F. Deng, E. Jovanov, H. Song, W. Shi, Y. Zhang, and W. Xu, "Wildar: Wifi signal-based lightweight deep learning model for human activity recognition," *IEEE Internet of Things Journal*, 2023.
- [10] Z. Chen, L. Zhang, C. Jiang, Z. Cao, and W. Cui, "Wifi csi based passive human activity recognition using attention based blstm," *IEEE Transactions on Mobile Computing*, vol. 18, no. 11, pp. 2714–2724, 2018.
- [11] J. Yang, H. Zou, Y. Zhou, and L. Xie, "Learning gestures from wifi: A siamese recurrent convolutional architecture," *IEEE Internet of Things Journal*, vol. 6, no. 6, pp. 10763–10772, 2019.
- [12] F. Wang, W. Gong, and J. Liu, "On spatial diversity in wifi-based human activity recognition: A deep learning-based approach," *IEEE Internet of Things Journal*, vol. 6, no. 2, pp. 2035–2047, 2018.
- [13] H. Zou, Y. Zhou, J. Yang, H. Jiang, L. Xie, and C. J. Spanos, "DeepSense: Device-free human activity recognition via autoencoder long-term recurrent convolutional network," in *2018 IEEE International Conference on Communications (ICC)*. IEEE, 2018, pp. 1–6.
- [14] B. Li, W. Cui, W. Wang, L. Zhang, Z. Chen, and M. Wu, "Two-stream convolution augmented transformer for human activity recognition," in *Proceedings of the AAAI Conference on Artificial Intelligence*, vol. 35, no. 1, 2021, pp. 286–293.
- [15] W. Jiang, C. Miao, F. Ma, S. Yao, Y. Wang, Y. Yuan, H. Xue, C. Song, X. Ma, D. Koutsonikolas *et al.*, "Towards environment independent device free human activity recognition," in *Proceedings of the 24th annual international conference on mobile computing and networking*, 2018, pp. 289–304.
- [16] F. Wang, J. Liu, and W. Gong, "Wicar: Wifi-based in-car activity recognition with multi-adversarial domain adaptation," in *Proceedings of the International Symposium on Quality of Service*, 2019, pp. 1–10.
- [17] Z. Wang, S. Chen, W. Yang, and Y. Xu, "Environment-independent wi-fi human activity recognition with adversarial network," in *ICASSP 2021-2021 IEEE International Conference on Acoustics, Speech and Signal Processing (ICASSP)*. IEEE, 2021, pp. 3330–3334.
- [18] Z. Zhou, F. Wang, J. Yu, J. Ren, Z. Wang, and W. Gong, "Target-oriented semi-supervised domain adaptation for wifi-based har," in *IEEE INFOCOM 2022-IEEE Conference on Computer Communications*. IEEE, 2022, pp. 420–429.
- [19] M. Long, Y. Cao, J. Wang, and M. Jordan, "Learning transferable features with deep adaptation networks," in *International conference on machine learning*. PMLR, 2015, pp. 97–105.
- [20] J. Liang, R. He, Z. Sun, and T. Tan, "Aggregating randomized clustering-promoting invariant projections for domain adaptation," *IEEE transactions on pattern analysis and machine intelligence*, vol. 41, no. 5, pp. 1027–1042, 2018.
- [21] B. Sun and K. Saenko, "Deep coral: Correlation alignment for deep domain adaptation," in *Computer Vision—ECCV 2016 Workshops: Amsterdam, The Netherlands, October 8–10 and 15–16, 2016, Proceedings, Part III 14*. Springer, 2016, pp. 443–450.
- [22] P. Koniusz, Y. Tas, and F. Porikli, "Domain adaptation by mixture of alignments of second-or higher-order scatter tensors," in *Proceedings of the IEEE conference on computer vision and pattern recognition*, 2017, pp. 4478–4487.
- [23] Y. Ganin, E. Ustinova, H. Ajakan, P. Germain, H. Larochelle, F. Laviolette, M. Marchand, and V. Lempitsky, "Domain-adversarial training of neural networks," *The journal of machine learning research*, vol. 17, no. 1, pp. 2096–2030, 2016.
- [24] Z. Luo, Y. Zou, J. Hoffman, and L. F. Fei-Fei, "Label efficient learning of transferable representations across domains and tasks," *Advances in neural information processing systems*, vol. 30, 2017.
- [25] T. M. H. Hsu, W. Y. Chen, C.-A. Hou, Y.-H. H. Tsai, Y.-R. Yeh, and Y.-C. F. Wang, "Unsupervised domain adaptation with imbalanced cross-domain data," in *Proceedings of the IEEE International Conference on Computer Vision*, 2015, pp. 4121–4129.
- [26] Z. Cao, M. Long, J. Wang, and M. I. Jordan, "Partial transfer learning with selective adversarial networks," in *Proceedings of the IEEE conference on computer vision and pattern recognition*, 2018, pp. 2724–2732.
- [27] J. Zhang, Z. Ding, W. Li, and P. Ogunbona, "Importance weighted adversarial nets for partial domain adaptation," in *Proceedings of the IEEE conference on computer vision and pattern recognition*, 2018, pp. 8156–8164.
- [28] S. Li, C. H. Liu, Q. Lin, Q. Wen, L. Su, G. Huang, and Z. Ding, "Deep residual correction network for partial domain adaptation," *IEEE transactions on pattern analysis and machine intelligence*, vol. 43, no. 7, pp. 2329–2344, 2020.
- [29] Z. Cao, K. You, M. Long, J. Wang, and Q. Yang, "Learning to transfer examples for partial domain adaptation," in *Proceedings of the IEEE/CVF conference on computer vision and pattern recognition*, 2019, pp. 2985–2994.
- [30] J. Hu, H. Tuo, C. Wang, L. Qiao, H. Zhong, J. Yan, Z. Jing, and H. Leung, "Discriminative partial domain adversarial network," in *Computer Vision—ECCV 2020: 16th European Conference, Glasgow, UK, August 23–28, 2020, Proceedings, Part XXVII 16*. Springer, 2020, pp. 632–648.
- [31] X. Gu, X. Yu, J. Sun, Z. Xu *et al.*, "Adversarial reweighting for partial domain adaptation," *Advances in Neural Information Processing Systems*, vol. 34, pp. 14860–14872, 2021.
- [32] M. Arjovsky, S. Chintala, and L. Bottou, "Wasserstein generative adversarial networks," in *International conference on machine learning*. PMLR, 2017, pp. 214–223.
- [33] S. Yousefi, H. Narui, S. Dayal, S. Ermon, and S. Valaei, "A survey on behavior recognition using wifi channel state information," *IEEE Communications Magazine*, vol. 55, no. 10, pp. 98–104, 2017.
- [34] Y. Ganin and V. Lempitsky, "Unsupervised domain adaptation by back-propagation," in *International conference on machine learning*. PMLR, 2015, pp. 1180–1189.
- [35] I. Gulrajani, F. Ahmed, M. Arjovsky, V. Dumoulin, and A. C. Courville, "Improved training of wasserstein gans," *Advances in neural information processing systems*, vol. 30, 2017.
- [36] A. Baha'A, M. M. Almazari, R. Alazrai, and M. I. Daoud, "A dataset for wi-fi-based human activity recognition in line-of-sight and non-line-of-sight indoor environments," *Data in Brief*, vol. 33, p. 106534, 2020.
- [37] L. Jia, Y. Gu, K. Cheng, H. Yan, and F. Ren, "Beaware: Convolutional neural network (cnn) based user behavior understanding through wifi channel state information," *Neurocomputing*, 2020.
- [38] E. Tzeng, J. Hoffman, K. Saenko, and T. Darrell, "Adversarial discriminative domain adaptation," in *Proceedings of the IEEE conference on computer vision and pattern recognition*, 2017, pp. 7167–7176.
- [39] M. Long, Z. Cao, J. Wang, and M. I. Jordan, "Conditional adversarial domain adaptation," *Advances in neural information processing systems*, vol. 31, 2018.
- [40] Z. Cao, L. Ma, M. Long, and J. Wang, "Partial adversarial domain adaptation," in *Proceedings of the European conference on computer vision (ECCV)*, 2018, pp. 135–150.